Four-quadrant Zero-current-transition Converter-fed Dc Motor Drives for Electric Propulsion

T. W. Ching

Department of Electromechanical Engineering, University of Macau, twching@umac.mo

Abstract

In this paper, a new four-quadrant (4Q) soft-switching converter for dc motor drives, namely the 4Q zero-current-transition (4Q-ZCT) converter, with the capabilities of 4Q power flow, and ZCT switching profile for dc motor drives is proposed. It has some definite advantages over their hard-switching counterparts and other soft-switching converters. Both the turn-on and turn-off losses of main switches are significantly reduced, while the auxiliary switches can always operate with zero-current-switching (ZCS). It possesses the advantages of reduced switching stresses, minimum voltage and current stresses as well as minimum circulating energy during both the motoring and regenerating modes. It also offers simple circuit topology, minimum component count and low cost.

Keywords

soft-switching, zero-current-transition, dc motor drives

1. INTRODUCTION

Recently, a number of soft-switching techniques, providing zero-voltage-switching (ZVS) or zero-current-switching (ZCS) condition, have been successfully developed for switched-mode power supplies (SMPS) [Canesin and Barbi, 1997; Chau, 1994; Mao et al., 1997; Wei and Ioinovici, 1998; Zhang and Sen, 2003]. A general assumption is that converters for SMPS can be directly applied to dc motor drives. However, unlike SMPS, dc motor drives, especially those used in electric railways and battery-powered electric vehicles, desire frequent regenerative braking. During braking, the dc motor operates as a generator to convert kinetic energy into electrical energy, and the converter must allow for backward power flow to restore the electrical energy to the power network or battery system. Thus, the incorporation of soft-switching into regenerating braking is particularly desirable for electric railways and battery-powered electric vehicles.

A two-quadrant (2Q) dc chopper (see Figure 1 (a)) is preferred as it converts battery dc voltage to variable dc voltage during the motoring mode and revert the power flow during regenerative braking. Furthermore, 4Q dc choppers (see Figure 1 (b)) are employed for reversible and regenerative speed control of dc motors. Instead of using mechanical contactors to achieve reversible operation, the 4Q dc chopper can be employed so that motoring and regenerative braking in both forward and reversible operations are controlled electronically. Both 2Q and 4Q dc choppers are shown in Figure 2.

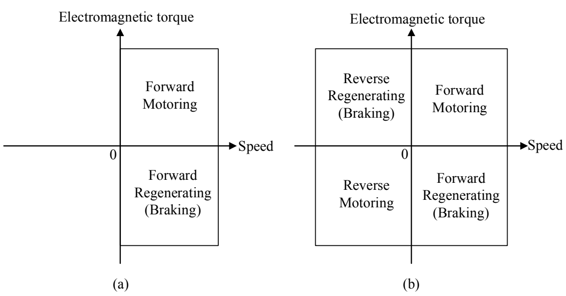

Fig. 1 Operation of a dc motor : (a) 2Q; (b) 4Q

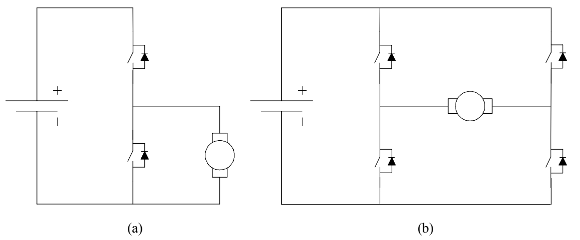

Fig. 2 Conventional dc choppers : (a) 2Q; (b) 4Q

Recently, two 2Q soft-switching dc-dc converters have purposely developed, namely the 2Q zero-voltage transition (2Q-ZVT) converter [Chau et al.,1999], and the 2Q-ZCT converter [Ching et al., 2001] for dc motor drives, which possess the advantages of high efficiency for both motoring and regenerative braking.

Very recently, a 4Q-ZVT converter has been developed for dc motor drives [Ching, 2005]. It possesses the advantages that all main transistors and rectifiers can switch with ZVS and unity device stresses during both the motoring and regenerating modes of operation.

Following the spirit of previous development on the 4Q-ZVT converter, the purpose of this paper is to propose a new 4Q-ZCT converter for dc motor drives. Differing from the 4Q-ZVT converter, this 4Q-ZCT converter takes the role to be particularly useful for those high-power dc motor applications, employing the IGBT as power devices, which generally suffer from diode reverse recovery during turn-on and severe inductive turn-off switching losses. It also possesses the advantages of high efficiency for both motoring and regenerative braking, as well as minimum voltage and current stresses. Its principle of operation, computer simulation and experimental results will be given.

2. PROPOSED 4Q-ZCT CONVERTER

Figure 3 shows the schematic diagram of the proposed 4Q-ZCT converter for dc motor drives. To achieve ZCS operation, two resonant tanks are required. Firstly, a resonant inductor L_a, resonant capacitor C_a, auxiliary switches S_a and $S_{a'}$ are added to allow for soft switching S_1 and S_4. Secondly, resonant inductor L_b, resonant capacitor C_b, auxiliary switches S_b and $S_{b'}$ are added to allow for soft switching S_2 and S_3. The dc motor can be considered to be simultaneously fed by two 2Q-ZCT converters.

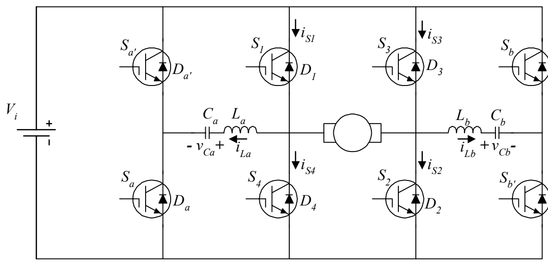

Fig. 3 Proposed 4Q-ZCT converter

The proposed ZCT converter operates in four modes (Figure 1(b)) :
- Forward motoring mode (Figures 4 to 6),
- Forward regenerating mode (Figures 7 to 9),
- Reverse motoring mode (Figures 10 to 12), and
- Reverse regenerating mode (Figures 13 to 15).

Their corresponding equivalent circuits and operating waveforms are shown in Figures 4 to 15. It can be found that all equivalent circuits involve nine operating stages (S1 to S9) within one switching cycle.

2.1 Forward motoring operation of ZCT converter (see Figures 4 to 6)

(a) Stage 1 [T_0-T_1]: S_a and S_b are turned on with ZCS at T_0. L_a, C_a and L_b, C_b start resonating. i_{La} increases from zero to peak, then decreases towards zero, (i_{Lb} decreases from zero to negative peak, then increases towards zero) and then change their direction. This stage finishes at T_1 when i_{La} reaches $-I_1$ (i_{Lb} reaches I_1) so that D_3 and D_4 become off.

(b) Stage 2 [T_1-T_2]: S_a and S_b are turned off while S_1 and S_2 are turned on with ZCS at T_1. The current of D_3 and D_4 are directed to the auxiliary circuit. i_{La} increases (i_{Lb} decreases) rapidly towards zero. This stage finishes at T_2 when i_{La} and i_{Lb} reach zero.

(c) Stage 3 [T_2-T_3]: Since i_{La} becomes positive (i_{Lb} becames negative) at T_2. D_a and D_b are off while $D_{a'}$ and $D_{b'}$ become on. $L_{a'}$, C_a and $L_{b'}$, C_b continue resonating. When i_{La} and i_{Lb} return to zero at T_3 , $D_{a'}$ and $D_{b'}$ turn off naturally.

(d) Stage 4 [T_3-T_4]: It is a forward powering stage. V_g is directly connected to the I_1 via S_1 and S_2.

(e) Stage 5 [T_4-T_5]: S_a and S_b are turned on with ZCS. $L_{a'}$, C_a and $L_{b'}$, C_b start resonating. i_{La} increases from zero to peak, then decreases towards zero (i_{Lb} decreases from zero to negative peak, then increases towards zero), and then change their direction. When they reach $-I_1$ and I_1 respectively at T_5, D_a and D_b become on.

(f) Stage 6 [T_5-T_6]: S_1 and S_2 are turned off with ZCS at T_5. As i_{La} keeps decreasing, its negative surplus flows

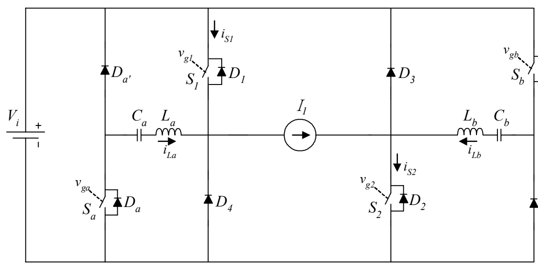

Fig. 4 Equivalent circuit during forward motoring mode

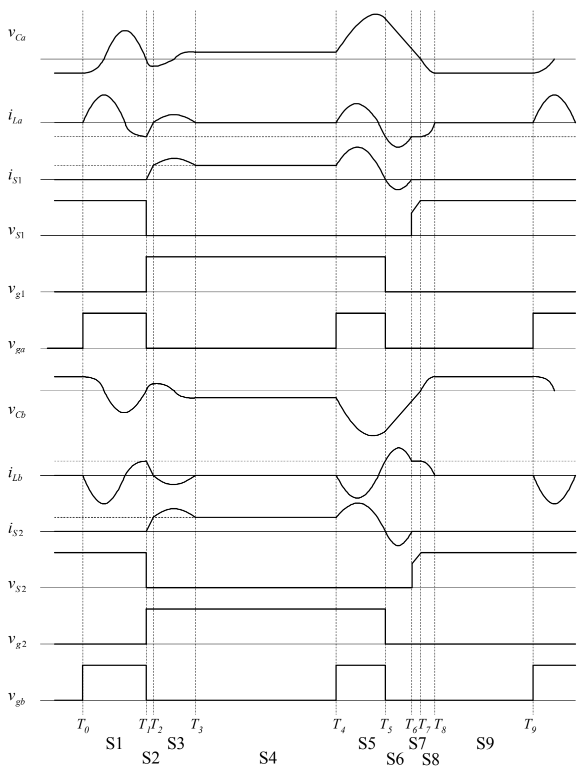

Fig. 5 Key waveforms during forward motoring mode

through D_1 (i_{Lb} keeps increasing, its surplus flows through D_2). At T_6, i_{La} and i_{Lb} swing back to $-I_1$ and I_1 respectively, D_1 and D_2 stop conducting.

(g) Stage 7 [T_6-T_7]: i_{La} keeps at $-I_1$ and v_{Ca} is linearly discharged towards zero, while i_{Lb} keeps at I_1 and v_{Cb} is linearly discharged towards zero. This stage ends at T_7 when v_{Ca} and v_{Cb} reach zero.

(h) Stage 8 [T_7-T_8]: At T_7, D_3 and D_4 start to conduct. L_a, C_a and L_b, C_b resonate again and i_{La} and i_{Lb} reach zero at T_8.

(i) Stage 9 [T_8-T_9]: I_1 is freewheeling via D_3 and D_4.

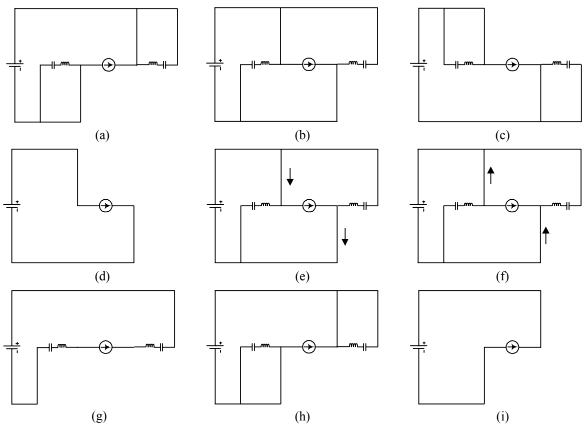

Fig. 6 Nine topological stages during forward motoring mode

2.2 Forward regenerating (braking) operation of ZCT converter (see Figures 7 to 9)

(a) Stage 1 [T_0-T_1]: $S_{a'}$ is turned on with ZCS. L_a and C_a start resonating. When i_{La} decreases from zero to negative peak, then increases towards zero, and then changes its direction. i_{La} reaches I_2 at T_1 and D_1 becomes off.

(b) Stage 2 [T_1-T_2]: Both $S_{a'}$ is turned off with ZCS and S^4 is turned on with ZCS at T_1. i_{La} decreases towards zero. This stage finishes at T_2 when i_{La} reaches zero.

(c) Stage 3 [T_2-T_3]: Since i_{La} becomes negative at T_2. The antiparallel diode of $S_{a'}$ is off while D_a becomes on. L_a and C_a continue resonating. i_{La} returns to zero while D_a is turned off naturally at T_3.

(d) Stage 4 [T_3-T_4]: I_2 is freewheeling via S_4.

(e) Stage 5 [T_4-T_5]: $S_{a'}$ is turned on with ZCS. L_a and C_a start resonating. i_{La} decreases from zero to negative peak, then increases towards zero, and then changes its direction. When it reaches I_2 at T_5, D_4 becomes on.

(f) Stage 6 [T_5-T_6]: S_4 is turned off with ZCS at T_5. As i_{La} keeps increasing, its surplus flows through D_4. At T_6, i_{La} swings back to I_2 and D_4 stops conducting.

(g) Stage 7 [T_6-T_7]: i_{La} keeps at I_2 and v_{Ca} is linearly discharged towards zero. This stage ends at T_7 when v_{Ca} reaches zero.

(h) Stage 8 [T_7-T_8]: At T_7, D_1 starts to conduct. L_a and C_a resonate again and i_{La} reaches zero at T_8.

(i) Stage 9 [T_8-T_9]: It is a regenerating stage via D_1 and D_2.

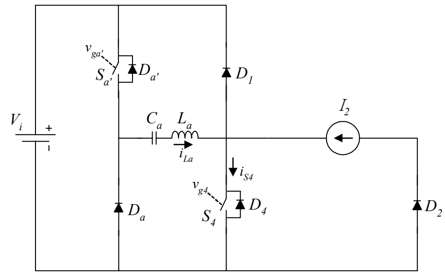

Fig. 7 Equivalent circuit during forward regenerating (braking) mode

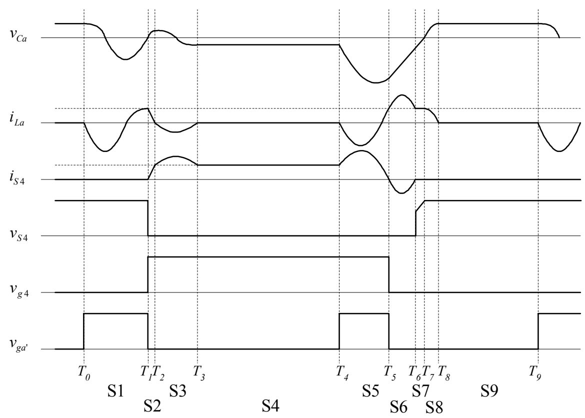

Fig. 8 Key waveforms during forward regenerating (braking) mode

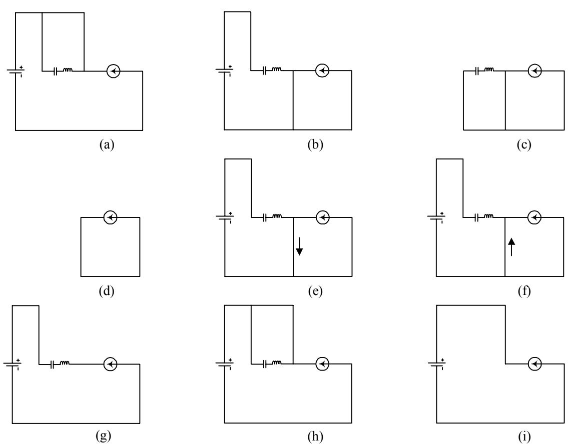

Fig. 9 Nine topological stages during forward regenerating (braking) mode

2.3 Reverse motoring operation of ZCT converter (see Figures 10 to 12)

(a) Stage 1 [T_0-T_1]: $S_{a'}$ and $S_{b'}$ are turned on with ZCS at T_0. L_a, C_a and L_b, C_b start resonating. i_{La} decreases from zero to negative peak, then increases towards zero, (i_{Lb} increases from zero to peak, then decreases towards zero) and then changes their direction. This stage finishes at T_1 when i_{La} reaches I_3 (i_{Lb} reaches $-I_3$) so that D_1 and D_2 become off.

(b) Stage 2 [T_1-T_2]: $S_{a'}$ and $S_{b'}$ are turned off while S_3 and S_4 are turned on with ZCS at T_1. The current of D_1 and D_2 are directed to the auxiliary circuit. i_{La} decreases (i_{Lb} increases) rapidly towards zero. This stage finishes at T_2 when i_{La} and i_{Lb} reach zero.

(c) Stage 3 [T_2-T_3]: Since i_{La} becomes negative (i_{Lb} becames positive) at T_2. $D_{a'}$ and $D_{b'}$ are off while D_a and D_b become on. L_a, C_a and L_b, C_b continue resonating. When i_{La} and i_{Lb} return to zero at T_3, D_a and D_b turn off naturally.

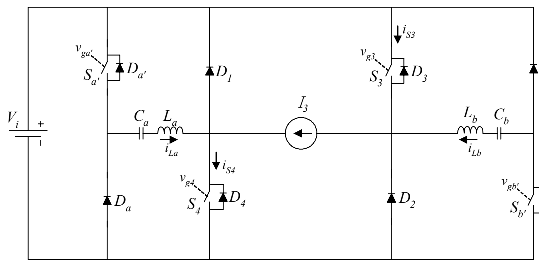

Fig. 10 Equivalent circuit during reverse motoring mode

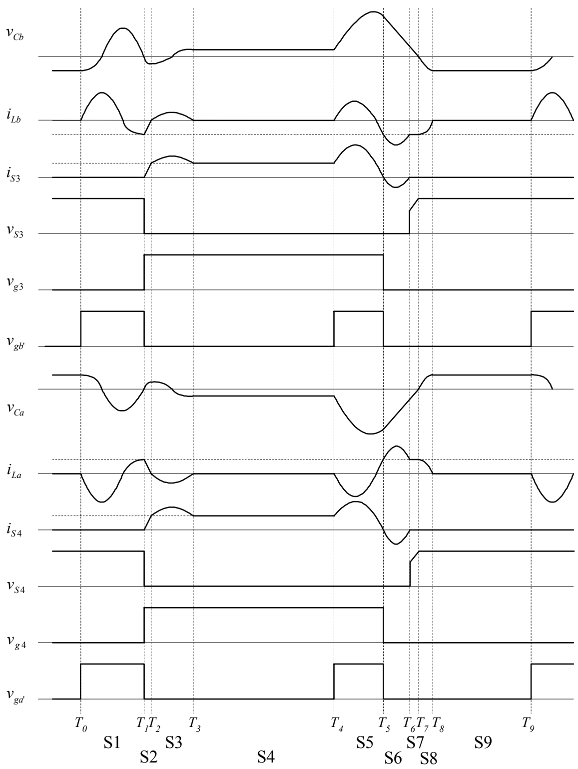

Fig. 11 Key waveforms during reverse motoring mode

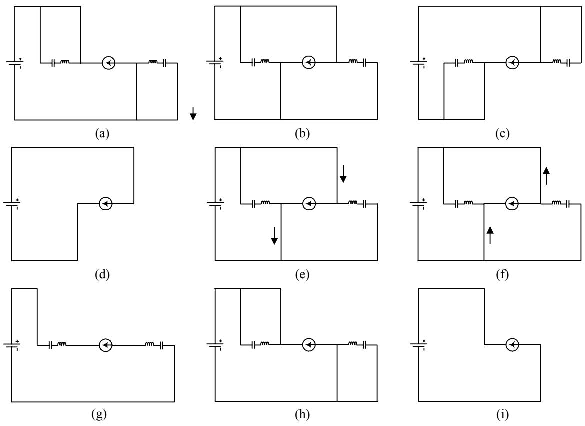

Fig. 12 Nine topological stages during reverse motoring mode

(d) Stage 4 [T_3-T_4]: It is a reverse powering stage. V_g is directly connected to the I_3 via S_3 and S_4.

(e) Stage 5 [T_4-T_5]: $S_{a'}$ and $S_{b'}$ are turned on with ZCS. L_a, C_a and L_b, C_b start resonating. i_{La} decreases from zero to negative peak, then increases towards zero (i_{Lb} from zero to peak, then decreases towards zero), and then change their direction. When they reach I_3 and $-I_3$ respectively at T_5, $D_{a'}$ and $D_{b'}$ become on.

(f) Stage 6 [T_5-T_6]: S_3 and S_4 are turned off with ZCS at T_5. As i_{La} keeps increasing, its surplus flows through D3 (i_{Lb} keeps decreasing, its surplus flows D_4). At T_6, i_{La} and i_{Lb} swing back to I_3 and $-I_3$ respectively, D_3 and D_4 stop conducting.

(g) Stage 7 [T_6-T_7]: i_{La} keeps at I_3 and v_{Ca} is linearly discharged towards zero, while i_{Lb} keeps at $-I_3$ and v_{Cb} is linearly discharged towards zero. This stage ends at T_7 when v_{Ca} and v_{Cb} reach zero.

(h) Stage 8 [T_7-T_8]: At T_7, D_1 and D_2 start to conduct. L_a, C_a and L_b, C_b resonate again and i_{La} and i_{Lb} reach zero at T_8.

(i) Stage 9 [T_8-T_9]: I_3 is freewheeling via D_1 and D_2.

2.4 Reverse regenerating (braking) operation of ZCT converter (see Figures 13 to 15)

(a) Stage 1 [T_0-T_1]: $S_{b'}$ is turned on with ZCS at T_0. L_b and C_b start resonating. i_{Lb} decreases from zero to negative peak, then increases towards zero and then changes its direction. This stage finishes at T_1 when i_{Lb} reaches I_4 so that D_3 become off.

(b) Stage 2 [T_1-T_2]: $S_{b'}$ is turned off while S_2 is turned on with ZCS at T_1. The current of D_3 is directed to the auxiliary circuit. i_{Lb} decreases rapidly towards zero. This stage finishes at T_2 when i_{Lb} reach zero.

(c) Stage 3 [T_2-T_3]: Since i_{Lb} becomes negative at T_2. $D_{b'}$ is off while D_b become on. L_b and C_b continue resonating. When i_{Lb} return to zero at T_3, D_b turn off naturally.

(d) Stage 4 [T_3-T_4]: It is freewheeling stage.

(e) Stage 5 [T_4-T_5]: $S_{b'}$ is turned on with ZCS. L_b and C_b start resonating. i_{Lb} decreases from zero to negative peak, then increases towards zero, and then change its direction. When it reaches I_4 at T_5, $D_{b'}$ becomes on.

(f) Stage 6 [T_5-T_6]: S_2 is turned off with ZCS at T_5. As i_{Lb} keeps increasing, its surplus flows through D_2. At T_6, i_{Lb} swing back to I_4, D_2 stop conducting.

(g) Stage 7 [T_6-T_7]: i_{Lb} keeps at I_4 and v_{Ca} is linearly discharged towards zero. This stage ends at T_7 when v_{Cb} reaches zero.

(h) Stage 8 [T_7-T_8]: At T_7, D_3 starts to conduct. L_b and C_b resonate again and i_{Lb} reach zero at T_8.

(i) Stage 9 [T_8-T_9]: It a reverse regenerating stage. V_g is directly connected to I_4 via D_3 and D_4.

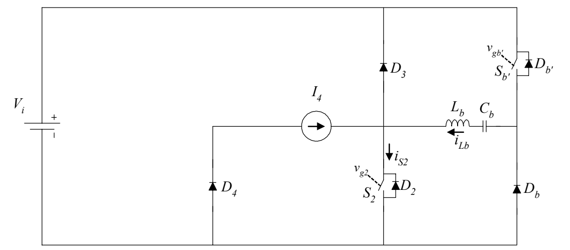

Fig. 13 Equivalent circuit during reverse regenerating (braking) mode

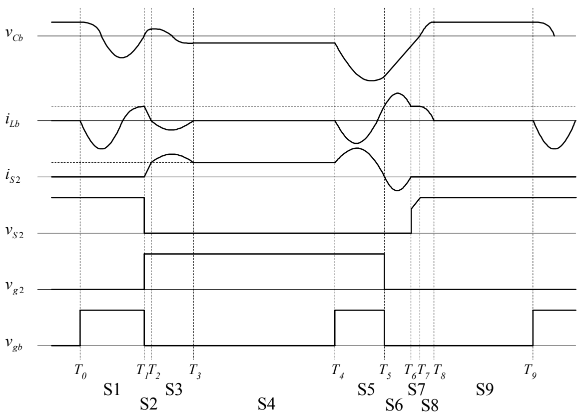

Fig. 14 Key waveforms during reverse regenerating (braking) mode

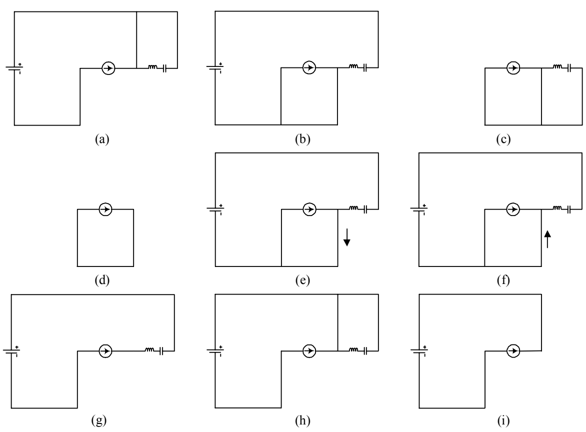

Fig. 15 Nine topological stages during reverse regenerating (braking) mode

3. SIMULATION AND VERIFICATION

Different modes of operation of the proposed 4Q-ZCT converter are PSpice-simulated. The corresponding results are shown in Figures 16 to 19.

Figure 16 shows the simulated waveforms of the proposed converter operating in the forward motoring mode. Both S_a and S_b are switched together to allow soft switching S_1 and S_2.

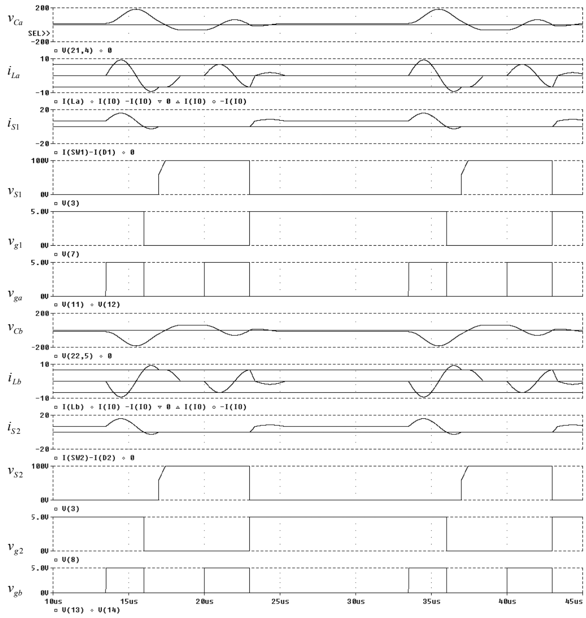

Fig. 16 PSpice simulation at forward motoring mode

Operating waveforms of the forward regenerating (braking) mode of the proposed converter is shown in Figure 17.

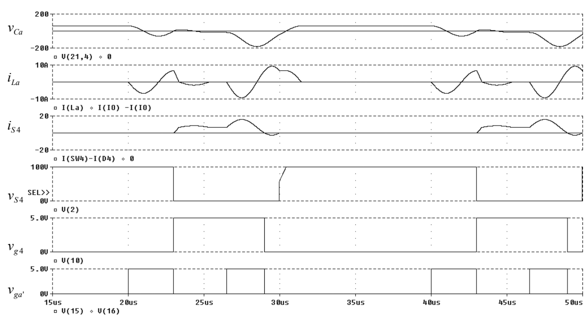

Fig. 17 PSpice simulation at forward regenerating (braking) mode

Figure 18 shows the operating waveforms of the 4Q-ZCT converter operating in reverse motoring mode. Both $S_{a'}$ and $S_{b'}$ are switched together to allow soft switching S_3 and S_4.

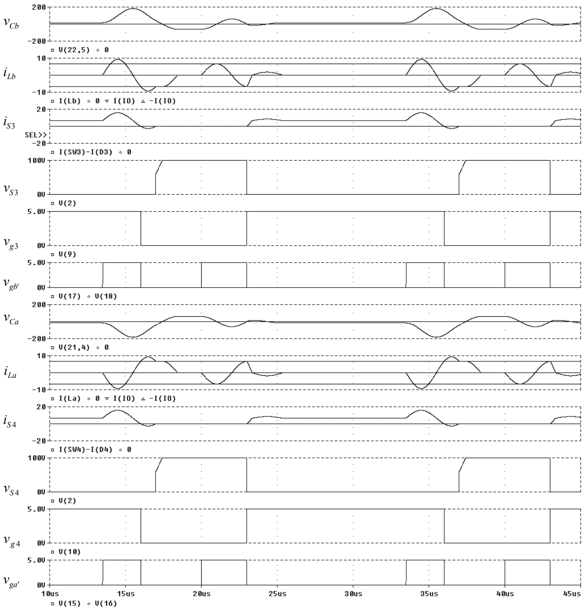

Fig. 18 PSpice simulation at reverse motoring mode

Operating waveforms of the proposed converter operating in reverse regenerating (braking) mode is shown in Figure 19.

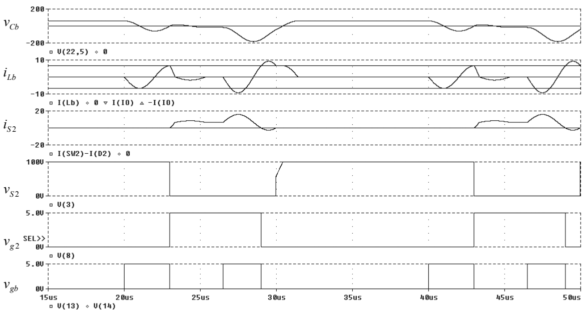

Fig. 19 PSpice simulation at reverse regenerating (braking) mode

The simulation results agree with those theoretical waveforms. The main and auxiliary switches can always maintain ZCS with minimum current and voltage stresses. To verify the theoretical results, the 4Q-ZCT converter is hardware prototyped as shown in Figure 20.

From the experimental waveforms shown in Figures 21 and 22, they also closely agree with those theoretical waveforms, the auxiliary switches can always maintain ZCS operation. The main switches can maintain ZCS during turn-on and turn-off. The resonant inductor current will be attenuated by the losses in the resonant tank, but still be very close to the load current. The turn-on

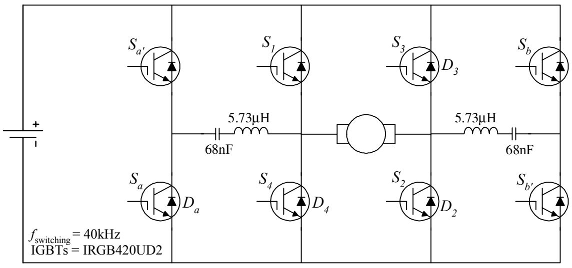

Fig. 20 Experimental 4Q-ZCT converter fed dc motor drive

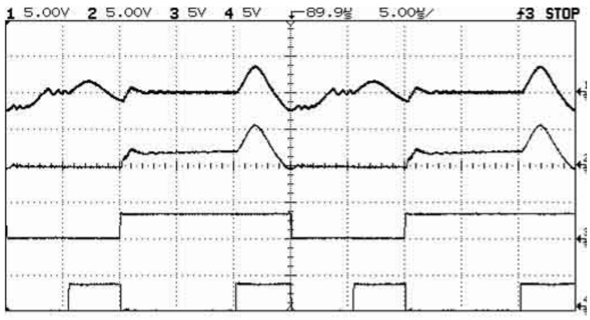

Fig. 21 Measured key waveforms at motoring (Duty Ratio=0.6); i_{La} (5A/div); i_{S1} (5A/div); v_{g1}, v_{ga} (5V/div)

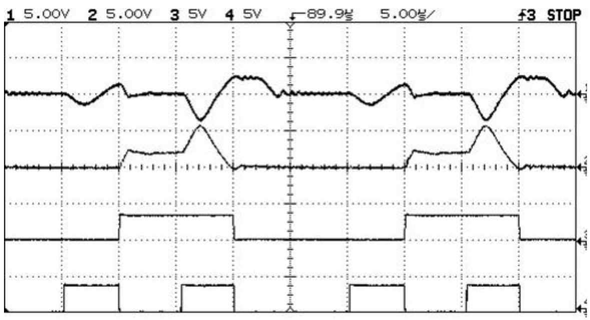

Fig. 22 Measured key waveforms at regenerating (Duty Ratio=0.4); i_{La} (5A/div); i_{S4} (5A/div); v_{g4}, $v_{ga'}$ (5V/div)

loss is significantly reduced by lowering the rise rate of diode reverse recovery.

To illustrate the gain in efficiency of the proposed converter, the efficiencies with and without using ZCT for both motoring and regenerating modes are plotted in Figure 23. The auxiliary resonant branches are removed to compare the performance of the proposed converter, the circuit efficiency is improved by 2-4% and 1-3% for motoring and regenerating modes respectively. Moreover, as shown in Figure 23, the measured efficiency (η) of the proposed converter is quite high, ranging from 87% to 96%. It should be noted that the IGBT main switches fail to work under hard-switching, due to the voltage over-shoot and subsequent thermal breakdown, when motoring over 400W. It indicates that the proposed ZCT circuit can effectively extend the operating range of the converter.

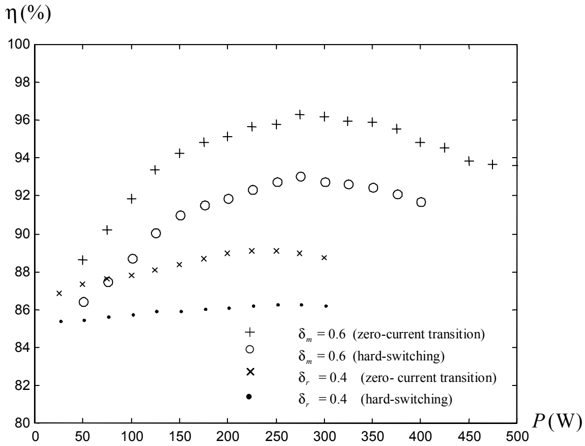

Fig. 23 Measured efficiency (η) at both motoring and regenerating

4. CONCLUSION

The principle of operation, characteristics, computer simulation and experimental results of a novel 4Q-ZCT converter for dc motor drives has been presented. It possesses some definite advantages: both turn-on and turn-off losses of main switches are significantly reduced, the auxiliary switches can always achieve ZCS, while the corresponding device voltage and current stresses are kept minimum. Moreover, the proposed converter provides reduced switching losses and stresses, minimum voltage and current stresses, minimum circulating energy, simple circuit topology and low cost, leading to achieve high power density and high efficiency. Other key features are the use of the same resonant tank for both forward and backward power flows and the full utilization of all diodes of the power switch packages, thus minimizing the overall hardware count and cost.

References

Canesin, C. A., and I. Barbi, Novel Zero-Current-Switching PWM Converters, *IEEE Transactions on Industrial Electronics*, Vol. 44, 372-381, 1997.

Chau, K. T., A New Class of Pulsewidth-Modulated Multi-Resonant Converters Using Resonant Inductor Freewheeling, *International Journal of Electronics*, Vol. 77, 703-714, 1994.

Chau, K. T., T. W. Ching, and C. C. Chan, A New Two-Quadrant Zero-Voltage Transition Converter for Dc Motor Drives, *International Journal of Electronics*, Vol. 86, 217-231, 1999.

Ching, T. W., and K. T. Chau, A New Two-Quadrant Zero-Current Transition Converter for Dc Motor Drives, *International Journal of Electronics*, Vol. 88, 719-735, 2001.

Ching, T. W., Four-quadrant Zero-voltage-transition Converter-fed DC Motor Drives for Electric Propulsion, *Journal of Asian Electric Vehicles*, Vol. 3, No. 2, 651-656, 2005.

Mao, H., F.C.Y. Lee, X. Zhou, H. Dai, M. Cosan, and D. Boroyevich, Improved Zero-Current Transition Converters for High Power Applications, *IEEE Transactions on Industry Applications*, Vol. 33, 1220-1231, 1997.

Wei, H., and A. Ioinovici, Zero-Voltage Transition Converter with High Efficiency Operating at Constant Switching Frequency, *IEEE Transactions on Circuits and Systems-I: Fundamental Theory and Applications*, Vol. 45, 1121-1128, 1998.

Zhang, Y., and P. C. Sen, A New Soft-Switching Technique for Buck, Boost, and Buck-Boost Converters, *IEEE Transactions on Industry Applications*, Vol. 39, 1775-1782, 2003.

(Received June 21, 2006; accepted August 22, 2006)